Instability of a crack in a heated strip

M. Marder

Department of Physics and Center for Nonlinear Dynamics, The University of Texas, Austin, Texas 78712
(Received 17 May 1993)

Yuse and Sano [Nature (London) **362**, 329 (1993); **362**, 295 (1993)] have shown that a crack traveling in a thin glass plate under thermal stresses undergoes numerous instabilities. The primary instability is calculated using a theory of Cotterell and Rice [Int. J. Fracture **16**, 155 (1980)] and is shown to reflect the velocity-dependent fracture energy of glass.

In an experiment reminiscent of directional solidification, Yuse and Sano [1,2], have shown that a crack traveling in a thin glass plate with thermal stresses undergoes a reproducible sequence of instabilities. The experiment, shown in Fig. 1, is conducted by slowly pulling a glass plate from a hot region to a cold one, so that in effect a thermal gradient travels across a plate. The plate is seeded with a crack, which the stresses in the thermal gradient cause to move at the pulling speed. When the plate exceeds a critical velocity, which depends upon temperature but is on the order of 1 cm/sec, the crack stops traveling in a straight line and begins to oscillate. The goal of this paper is to calculate the conditions under which this first bifurcation occurs. The results can be used to find the fracture energy of glass as a function of crack velocity.

The glass strip in which the experiment is conducted is 0.01 cm thick. Since the thermal diffusion coefficient in glass is $D = 4.7 \times 10^{-3}$ cm^2/sec the thermal diffusion length $d_0 = D/v$ will be greater than the plate width so long as the velocity v at which the plate moves is less than 4.7 mm/sec. The experiment does proceed to velocities at which this relation is violated, but the offending regime will be left out of the analysis. It will be assumed that the temperature field is uniform throughout the 0.01 cm thickness of the plate, making the problem two dimensional. Since all such velocities are much slower than the speed of sound in glass, calculations will all be in the quasistatic limit.

Sufficiently near the. tip of a straight crack loaded symmetrically about the crack axis, the stress field takes
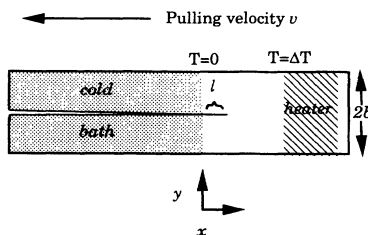
FIG. 1. Sketch of the experiment of Yuse and Sano, Ref. [1]. Successive figures in the vertical direction represent steady-state patterns achieved in successive experiments where the constant velocity v increases. At low sliding speeds a straight crack is stable, but it begins to oscillate at a critical speed. At yet higher velocities, the cracks become unstable to complicated branching patterns.

the universal form [3]

$$\sigma_{yy} = \frac{K_I}{\sqrt{2\pi r}} + O(\sqrt{r}) , \tag{1a}$$

$$\sigma_{xx} = \frac{K_I}{\sqrt{2\pi r}} + \Sigma + O(\sqrt{r}) , \tag{1b}$$

at a distance r from the crack tip, approaching along the line of the crack. K_I is a constant known as the stress intensity factor, setting the scale of singularity; Σ is an additional constant. In addition, the energy per unit area which flows to the crack tip as it extends is [4]

$$G = K_I^2(1-v^2)/E , \tag{2}$$

where v is the Poisson ratio and E is the Young modulus. In order to find out when the straight crack becomes unstable, one should carry out a perturbative calculation for a crack in a strip where the path of the crack deviates slightly from a straight line. This calculation can be carried out, but the results are complicated, and a simpler procedure will be adopted here. The stability of a crack in a sufficiently wide strip should be the same as the stability of a crack in an infinite plate. The only length to which one can compare the width of the strip $2b$, to determine when the infinite plate approximation might be appropriate, is the width of the region of rapid temperature change. In Yuse and Sano's experiment the thermal diffusion length d_0 is less than a millimeter, while the width of the strip $2b$ is 2.4 cm. For this reason, it is reasonable to pretend that the crack travels in an infinite plate for the purpose of determining its stability. The drawback in this procedure is that it does not allow one to calculate the wavelength of oscillations once the bifurcation occurs. The advantage is that one can use a theory of Cotterell and Rice that makes the results conceptually simple.

Cotterell and Rice [5] have shown that for a crack traveling in an infinite plate, stability is determined completely by the constant stress Σ [Eq. (1)] which remains in the stress field near the tip of the crack after the leading square-root singularity has been subtracted out. If the constant Σ is positive, the crack will be unstable, and begin to deviate from straight motion, while if it is negative the crack will be stable. I will now proceed to the details of how to calculate K_I and Σ. The calculation will mainly be carried out in Fourier space, finding the large k behavior of the stresses. The qualitative structure of the

result can be understood entirely by reference to Fig. 2.

Under plane strain conditions, the strain tensor of a two-dimensional plate in a temperature field is related to the stress tensor by [6]

$$\epsilon_{xx} = \frac{1}{E}(\sigma_{xx} - \nu\sigma_{yy}) + \alpha_T T_l \ , \tag{3a}$$

$$\epsilon_{yy} = \frac{1}{E}(\sigma_{yy} - \nu\sigma_{xx}) + \alpha_T T_l \ , \tag{3b}$$

$$\epsilon_{xy} = \frac{2(1+\nu)}{E}\sigma_{xy} \ , \tag{3c}$$

where α_T is the linear coefficient of thermal expansion, and

$$T_l(x) = \Delta T(1 - e^{-(x+l)\nu/D})\theta(x+l) \tag{4}$$

is the temperature, measured relative to the temperature of the cold bath. The reason that the parameter l has been introduced is that it will be necessary to consider the stresses surrounding a crack whose tip is at an arbitrary location along the x axis relative to a given temperature field. It is most convenient to take the tip of the crack always to be at the origin, and displace the temperature field by $-l$.

A given set of strains can only result from displacements if it obeys the compatibility condition

$$\frac{\partial^2\epsilon_{xx}}{\partial y^2} + \frac{\partial^2\epsilon_{yy}}{\partial x^2} = \frac{\partial^2\epsilon_{xy}}{\partial x\,\partial y} \ . \tag{5}$$
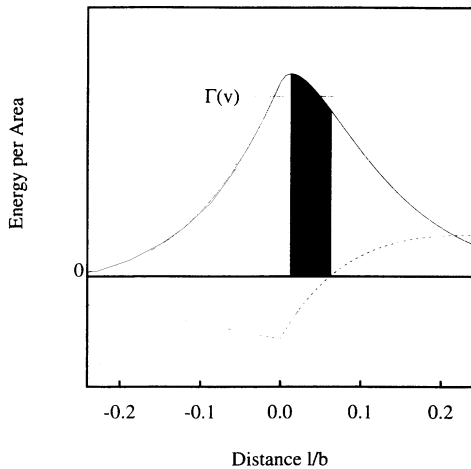
FIG. 2. The upper solid curve shows the energy available per unit length for crack propagation in the experiment of Yuse and Sano. The horizontal axis shows the position of the crack tip relative to the cold end of the temperature gradient, and is measured in units of the half-width of the plate b. The scale of the vertical axis is not indicated, but the only important fact is that the vertical scale is proportional to the square of the temperature difference ΔT along the strip. The crack will propagate with its tip at a spatial location given by the intersection of the solid curve with the dashed line labeled $\Gamma(v)$. The lower dotted line monitors the stress field Σ responsible for the stability of the crack. When the crack tip reaches the spatial location where this quantity is positive, it becomes unstable; the shaded region indicates the range of stable crack position.

Placing Eq. (3) into Eq. (5) and using the equations of force balance

$$\frac{\partial}{\partial\alpha}\sigma_{\alpha\beta} = 0 \tag{6}$$

gives

$$\nabla^2(\sigma_{xx} + \sigma_{yy}) = -E\alpha_T\nabla^2 T_l \ . \tag{7}$$

Writing the stresses in terms of the Airy stress function ϕ, such that

$$\sigma_{xx} = \frac{\partial^2\phi}{\partial y^2} \ , \quad \sigma_{yy} = \frac{\partial^2\phi}{\partial x^2} \ , \quad \phi_{xy} = -\frac{\partial^2\phi}{\partial x\,\partial y} \ , \tag{8}$$

one has finally that

$$\nabla^2\nabla^2\phi = -E\alpha_T\nabla^2 T_l \ . \tag{9}$$

Fourier transforming in the x direction, Eq. (9) becomes

$$\left[k^4 - 2k^2\frac{\partial^2}{\partial y^2} + \frac{\partial^4}{\partial y^4}\right]\phi = Ek^2\alpha_T T_l(k) \ . \tag{10}$$

One has that

$$u_y = \left\{2\epsilon_{xy} + \frac{\partial}{\partial y}\left[\frac{\epsilon_{xx}}{ik}\right]\right\}\bigg/(-ik) \tag{11}$$

and the boundary conditions

$$\sigma_{xy} = \sigma_{yy} = 0 \quad \text{at } y = b \ , \tag{12a}$$

$$\sigma_{xy} = 0 \ , \quad u_y = u_y^0 \quad \text{at } y = 0 \ . \tag{12b}$$

Solving Eq. (10) using Eq. (11) and Eq. (12) one finds for the stresses σ_{xx}^0 and σ_{yy}^0 (where the superscript indicates that they are evaluated at $y = 0$)

$$\sigma_{yy}^0 = -F(k)u_y^0 + D_l(k) \ , \tag{13a}$$

$$\sigma_{xx}^0 = H(k)\sigma_{yy}^0 + S_l(k) \ , \tag{13b}$$

with

$$F(k) = \frac{E}{2}k\frac{\sinh^2 bk - b^2 k^2}{\cosh bk \ \sinh bk + bk} \ , \tag{14}$$

$$D_l(k) = E\alpha_T T_l(k)\frac{(1 - \cosh bk)(\sinh bk - bk)}{\cosh bk \ \sinh bk + bk} \ , \tag{15}$$

$$H(k) = \frac{\sinh^2 bk + b^2 k^2}{\sinh^2 bk - b^2 k^2} \ , \tag{16}$$

and

$$S_l(k) = E\alpha_T T_l(k)\frac{\sinh^2 bk + b^2 k^2 - 2bk \ \sinh bk}{\sinh^2 bk - b^2 k^2} \ . \tag{17}$$

At this point, one invokes the presence of the crack with the conditions that at $y = 0$, σ_{yy} vanishes for $x < 0$, and u_y vanishes for $x > 0$. Writing $F(k) = F^-/F^+$, where $F^-(k)$ has neither zeros nor poles for $\text{Im}(k) < 0$, and $F^+(k)$ has none for $\text{Im}(k) > 0$, one finds from the Wiener-Hopf method [7,8]

$$\sigma_{yy}^0(k) = \frac{1}{F^+(k)}\int dx \ e^{ikx}\theta(x)f(x+l) \ , \tag{18}$$

with

$$f(l)= \int \frac{dk'}{2\pi} e^{-ik'l} D_0(k')F^+(k') . \tag{19}$$

One can choose the large k behavior of $F^+(k)$ to be

$$\lim_{k\to\infty} F^+ \to 1/\sqrt{\delta-ik} , \tag{20}$$

with δ infinitesimal. The large k behavior of σ_{yy}^0 is set by the fact that the integrand in Eq. (18) is discontinuous at $x=0$, so that

$$\lim_{k\to\infty} \sigma_{yy}^0 \to \sqrt{\delta-ik}\, \frac{f(l)}{\delta-ik} . \tag{21}$$

The coefficient K_I appearing in Eq. (1) is then found from

$$K_I = \lim_{k\to\infty} \sqrt{2(\delta-ik)}\sigma_{yy}^0 = \sqrt{2}f(l) . \tag{22}$$

Let $\tilde{K}_I$ be the constant found numerically [9] by setting $b=1$, and $E\alpha_T\Delta T=1$ in Eq. (15) and Eq. (19). Dimensions return to the problem as

$$K_I = E\alpha_T\Delta T\sqrt{b}\,\tilde{K}_I . \tag{23}$$

The energy release per unit crack extension is then

$$G =(1-v^2)\alpha_T^2 Eb\,(\Delta T)^2\tilde{K}_I^2 = \Gamma(v) . \tag{24}$$

The final equality introduces the fracture energy $\Gamma(v)$, which is the amount of energy needed per unit area to form new fracture surfaces. The fracture energy $\Gamma(v)$ is a property of the material, and the dynamics of crack motion must adjust themselves so that Eq. (24) holds.

The calculation of Σ can easily be carried out from Eq. (13b); the first term on the right-hand side produces the dominant square-root singularity seen in Eq. (1) but has no constant term associated with it; the constant Σ can be found by Fourier transforming the second term on the right-hand side. This gives

$$\Sigma(l)= \int \frac{dk}{2\pi} S_0(k)e^{-ikl} . \tag{25}$$

One finds $\Sigma(l)$ for many crack tip locations l by carrying out a single fast Fourier transform in Eq. (25), having used Eq. (4).

The results of these calculations are summarized in Fig. 2. The solid line shows $\tilde{K}_I^2(l)$, calculated from Eq. (22). The dotted line shows $\Sigma(l)$, calculated from Eq. (25). The condition $\Gamma(v)=G$ is indicated in the figure by a dashed line. In particular, if at any given velocity the temperature gradient ΔT is increased, then G increases as the square of ΔT, so the location of the crack tip will be shoved forward. However, examining the dotted line, one sees that when pushed forward too far, the crack tip passes the location where $\Sigma=0$, and the crack becomes unstable. In fact, using Eq. (24), one can take the locus of experimental points where the instability is first observed and from it find $\Gamma(v)$. For any given velocity v, one calculates the temperature field from Eq. (4), the location l_c where $\Sigma(l)$ vanishes from Eq. (25), the stress singularity $\tilde{K}_I(l_c)$ at this location from Eq. (22), and finally turning
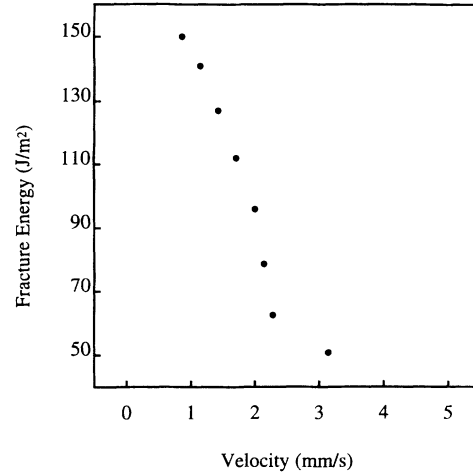
FIG. 3. Fracture energy as a function of velocity, deduced from Fig. 3 of Ref. [1]. At velocities approaching 5 mm/sec, three-dimensional effects are becoming important, and invalidate the theory in this paper, but I believe that the drop in fracture energy with velocity is real. Values used for evaluation of Eq. (24) are $E=7.23\times10^{10}$ J/m^3, $b=1.2$ cm, $\alpha_T=0.77\times10^{-5}$ K^{-1}, $D=4.7\times10^{-3}$ cm^2/sec, and $v=0.23$. Thus $\Gamma(v)=0.049(\tilde{K}_I\Delta T)^2$ J/m^2 K. Calculation finds that $\tilde{K}_I^2$ varies between 0.15 and 0.23 for velocities of the experiment, and a typical temperature drop is $\Delta T=100$ K. By way of comparison, the surface energy of soda-lime glass found by Griffith, Ref. [10], is 0.54 J/m^2, and the value of fracture energy Γ for borosilicate glass (the type used by Yuse and Sano) is around 10 J/m^2 (Ref. [11]).

to Eq. (24), $\Gamma(v)$.

The results of this calculation for the data of Yuse and Sano are contained in Fig. 3. As the velocity approaches 5 mm/sec, it becomes unreasonable to treat the problem as two dimensional, so the plot is not continued to that point. The values of fracture energy found here are about five times as large as those obtained by other methods, 10 J/m^2 [11]. However, Fig. 3 shows a very sharp drop in fracture energy with crack velocity, and if the points may be extrapolated, the standard result would correspond to the fracture energy at about 5 mm/sec. This drop should be hoped for, if not expected, since glass is a brittle material. Brittleness does not mean that a material is free of dissipation; there are substantial temperature rises near the tip of a crack in glass. Instead, it means that rapid acceleration is possible despite it. The drop in surface energy means that cracks exceeding at least 1 mm/sec will inevitably accelerate to much higher velocities under almost all loading conditions. Thermal loading is able to trap the crack in this highly unstable configuration, and reveal behavior of the fracture energy that would be invisible from other points of view.

[1] A. Yuse and M. Sano, Nature (London) **362**, 329 (1993).

[2] M. Marder, Nature (London) **362**, 295 (1993).

[3] L. B. Freund, *Dynamic Fracture Mechanics* (Cambridge University Press, New York, 1990), Sec. 4.3.

[4] L. B. Freund, Ref. [3], Sec. 5.3.

[5] B. Cotterell and J. R. Rice, Int. J. Fracture **16**, 155 (1980).

[6] S. Timoshenko and J. N. Goodier, *Theory of Elasticity,* 2nd ed. (McGraw-Hill, New York, 1951), Secs. 15, 16, and 137.

[7] W. G. Knauss, J. Appl. Mech. **33**, 356 (1966); also a comment and reply **34**, 248 (1967).

[8] B. Noble, *Methods Based on the Wiener-Hopf Technique for the Solution of Partial Differential Equations* (Pergamon, New York, 1958).

[9] The Wiener-Hopf decomposition needed for Eq. (19) is computed using the method described by Xiangming Liu and M. Marder, J. Mech. Phys. Solids **39**, 947 (1991). All other quantities are computed using fast Fourier transforms. It is always necessary to separate out singular parts of functions and treat them analytically, but there are no other difficulties.

[10] A. A. Griffith, Philos. Trans. R. Soc. London Ser. A **221**, 163 (1921).

[11] K. Reddy, E. H. Fontana, and J. D. Helfinstine, J. Am. Ceram. Soc. **71**, C310 (1988).

FIG. 1. Sketch of the experiment of Yuse and Sano, Ref. [1]. Successive figures in the vertical direction represent steady-state patterns achieved in successive experiments where the constant velocity v increases. At low sliding speeds a straight crack is stable, but it begins to oscillate at a critical speed. At yet higher velocities, the cracks become unstable to complicated branching patterns.